UDK 669.14.018.8
Original scientific article/Izvirni znanstveni članek

ISSN 1580-2949
MTAEC9, 56(6)613(2022)

STRENGTHENING MECHANISM OF 15-5PH STAINLESS STEEL UNDER DIFFERENT AGING TEMPERATURES

MEHANIZEM UTRJEVANJA NERJAVNEGA JEKLA VRSTE 15-5PH PO STARANJU PRI RAZLIČNIH TEMPERATURAH

Bei Li[1], Chunhui Jin[1], Guoqiang Li[1], Jinhua Zhao[1,2*], Jinshan Chen[3], Lifeng Ma[2]

[1]School of Materials Science and Engineering, Taiyuan University of Science and Technology, Taiyuan, China
[2]Heavy Machinery Engineering Research Center of the Ministry of Education, Taiyuan University of Science and Technology, Taiyuan, China
[3]College of Materials Science and Engineering, Nanjing Institute of Technology, Nanjing, China

Prejem rokopisa – received: 2022-06-23; sprejem za objavo – accepted for publication: 2022-09-20

doi:10.17222/mit.2022.535

The research described here was aimed at illuminating the variation in the strengthening mechanism of Cr15Ni5 precipitation hardening stainless steel (15-5PH stainless steel) processed at aging temperatures ranging from 440–610 °C. The variation in the tensile property corresponding to different aging processes was measured, and the microstructure features were further characterized using a transmission electron microscope (TEM) and electron back-scatter diffraction (EBSD). Results indicated that the strength contribution induced by grain-refinement strengthening, precipitation strengthening and dislocation strengthening corresponding to different aging temperatures varying from 470–610 °C were determined to be distributed in strength ranges of 296–345 MPa, 0–469 MPa and 97–803 MPa, respectively. The strength increments caused by different combinations of precipitation strengthening and dislocation strengthening were crucial for determining the final mechanical properties of the studied 15-5PH stainless steel.

Keywords: 15-5PH stainless steel, aging process, microstructure, strengthening mechanism

Članek opisuje mehanizem utrjevanja izločevalno utrjevalnega nerjavnega jekla vrste 15-5PH (Cr15Ni5), ki je bilo umetno starano v temperaturnem območju med 440 °C in 610 °C. V skladu z različnimi postopki staranja izbranega nerjavnega jekla so bile določene njegove mehanske lastnosti in mikrostruktura s presevnim elektronskim mikroskopom (TEM) in spektroskopijo na osnovi disperzije povratno sipanih elektronov (EBSD). Rezultati analiz so pokazali, da je posledica utrditve jekla udrobljenje oziroma zmanjšanje velikost kristalnih zrn, kot tudi dislokacijska utrditev v skladu z različnimi temperaturami (od 470 °C do 610 °C v korakih po 30 °C) umetnega staranja v razponih od 296 MPa do 345 MPa, od 0 do 469 MPa in od 97 MPa do 803 MPa. Prirastek trdnosti jekla je bil posledica različnih kombinacij izločevalnega in dislokacijskega utrjevanja, kar je bil tudi ključ do dokončne analize in določitve mehanskih lastnosti preučevanega nerjavnega jekla vrste 15-5PH.

Ključne besede: nerjavno jeklo vrste 15-5PH, process umetnega staranja, mikrostruktura, mehanizem utrjevanja

1 INTRODUCTION

Martensitic stainless steel (MSS) is the generic term for a type of stainless steel characterized by carbon-free or ultra-low carbon chemical composition design, whose ideal microstructure is generally composed of martensite with dispersed precipitates distributed across the matrix. Due to the comprehensive mechanical properties together with outstanding corrosion resistance, the MSS has been widely applied in the nuclear, chemical as well as aerospace industries.[1–3] The chemical composition of MSS has been generally designed considering the beneficial effects induced by different elements, such as a high amount of Cr for good corrosion resistance, a relatively low carbon addition for avoiding a generation of various kinds of carbides, and a certain volume fraction of Cu for precipitation formation.[2,3] Whether the potential of mechanical properties can be exploited in line with the actual requirements, mainly depends on whether the selection of the processing technology is reasonable with respect to MSS.

As an optimized MSS grade, Cr15Ni5 precipitation hardening stainless steel (15-5PH stainless steel) has drawn a great deal of attention from scholars due to its high potential for excellent comprehensive mechanical properties and corrosion resistance performance in case of a simple and convenient solution and aging treatment process.[4–7] For 15-5PH stainless steel, some studies focused on the effects of various heat-treatment processes on the microstructure evolution and mechanical property control have been performed and reported, and the corresponding strengthening mechanisms involved in the microstructural control have also been qualitatively discussed. For instance, D. Palanisamy et al.[4] revealed that a high yield strength at the aging treatment at 482 °C for 1 h could be achieved for 15-5 PH stainless steel due to the generation of Cu-enriched precipitates, and that the strength should be decreased to a lower value when the aging temperature was increased to 621 °C. S. Chenna Krishna et al.[5] comparatively investigated the microstructure and properties of 15-5PH stainless steel during different aging processes, and found that samples aged at

*Corresponding author's e-mail:
jhzhao2010@163.com (Jinhua Zhao)

250 °C for 2 h showed a low strength due to a reduction in internal stresses and a decrease in the dislocation density within the lath. On the other hand, a relative high strength could be obtained during an aging process at 500 °C for 2 h due to the precipitation hardening induced by fine precipitates distributed across the martensite matrix. C. H. Jin et al.[6] systematically investigated the evolution of the microstructure and mechanical properties under different aging processes for 15-5PH stainless steel, and the varying trend of the strengthening mechanisms was qualitatively discussed in terms of the experimental results. To summarize, the reported studies performed certain researches associated with the mechanical property control and qualitative illumination of the strengthening mechanism of 15-5PH stainless steel. On the other hand, a systematically quantified investigation associated with the strengthening mechanism of 15-5PH stainless steel was reported rarely, which restricted the understanding of the basic physical metallurgical behavior and further potential exploration of mechanical properties.

In the present study, the strength increments induced by different strengthening mechanisms were theoretically calculated for a typical 15-5PH stainless steel processed via different aging processes, and the change in the strengthening mechanism with the aging temperature was systematically and quantitatively illuminated and used as the theoretical reference for the microstructural regulation and exploitation of mechanical property potential of the 15-5PH stainless steel.

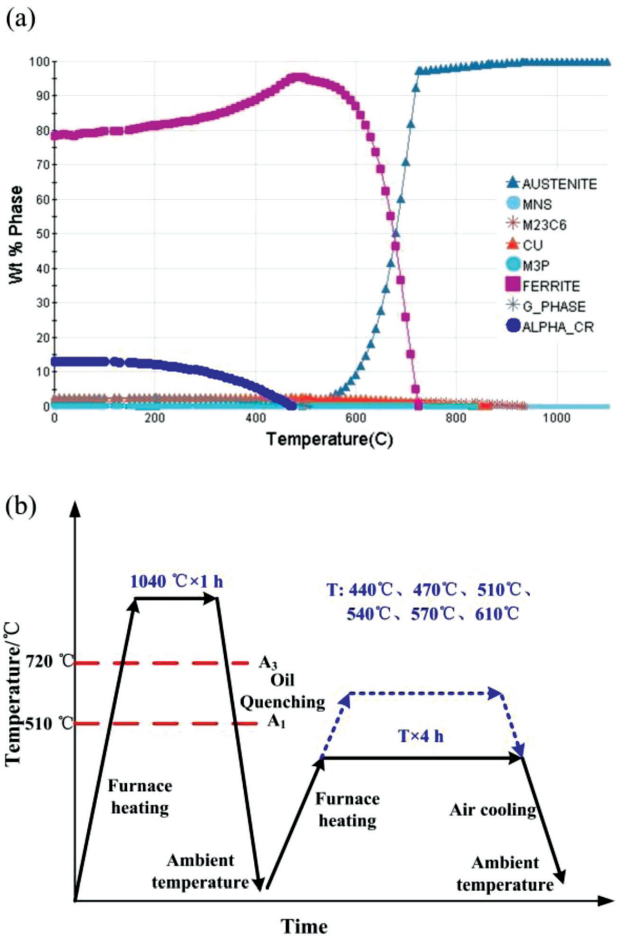

Figure 1: a) Equilibrium-phase diagram of the studied steel and b) schematic diagram of the heat treatment applied in the present study

2 EXPERIMENTAL PART

The steel used in the present study was 15-5PH stainless steel, and its chemical composition was 0.04 C, ≤ 1.00 Si, ≤ 1.0 Mn, 14.2 Cr, 3.5 Ni, 0.5 Mo+Nb, 2.5 Cu, ≤ 0.03 P, ≤ 0.01 S, ≤ 0.01 N, ≤ 0.01 O and a balance of Fe. An ingot of 50 kg was first fabricated using a vacuum induction furnace, and then it was forged into a 100-mm-thick slab using a hydraulic press with a maximum pressure of 500 t. To eliminate the elemental segregation formed during casting, homogenization annealing was carried out at 950 °C for 5 h, and the slab was then machined into samples with dimensions of (20 × 20 × 150) mm for the subsequent final heat treatment. To ensure that the dominant alloying elements could be fully dissolved into the iron matrix, the solution temperature and time were selected as 1040 °C and 1 h following a similar reference[8] and the equilibrium phase transition diagram of the studied steel calculated by utilizing thermo- dynaimc software JmatPro as shown in **Figure 1a**. Furthermore, the aging treatment time was determined to be 4 h considering the design purpose of the chemical composition and the reported paper[8] to ensure the effective precipitaiton of the Cu-enriched phase. In order to systematically present the variation in the strengthening mechanism as a function of the aging temperature, the aging temperature was confirmed to be in a range of 440–610 °C, indicating that the aging processes were performed both in the single-phase region and dual-phase region, including α and γ in line with the achieved equilibrium-phase transition diagram and the schematic diagram of the heat-treatment process given in **Figure 1b**.

After the heat treatment, the tensile-sample preparation and tensile test were carried out in accordance with the specification of China (No. GB/T 228.1-2010). To characterize the substructural features of the studied steel obtained under different aging processes, a substructure observation and nano-sized precipitate analysis were performed utilizing a transmission electron microscope (TEM, Model: JEM-2100). Specimens with a thickness of 500 μm were first mechanically polished to 40 μm and punched into discs with a diameter of 3 mm; samples were then thinned using twin-jet polishing with a solution consisting of 10 % of perchloric acid and 90 % of alcohol. To obtain the crystallographic information of the studied steel processed with different aging processes, an electron back-scatter diffraction (EBSD) analysis was carried out through scanning electron microscopy

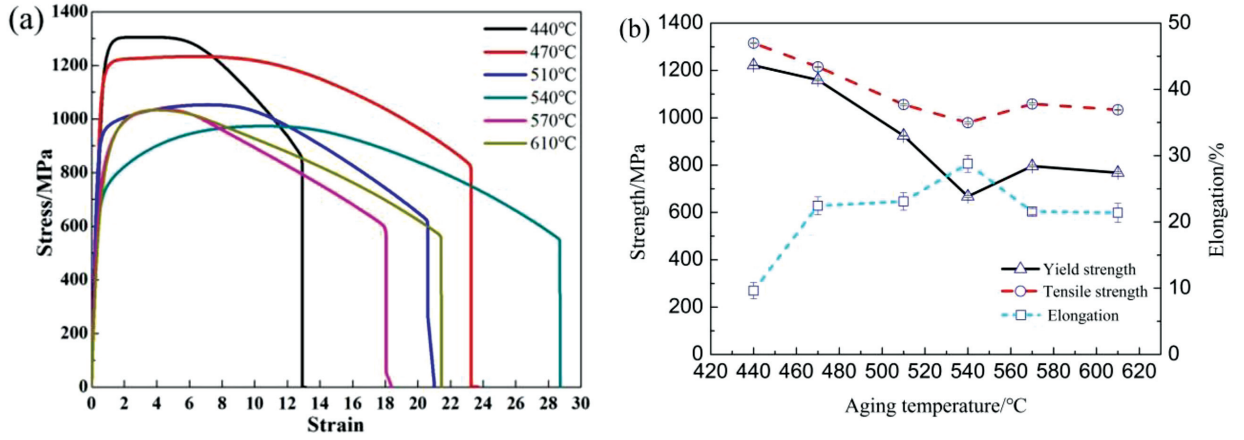

Figure 2: a) Tensile curves of the studied 15-5PH steel processed at different aging temperatures and b) varying trend of the strength and fracture elongation corresponding to different aging temperatures

(Model: ZEISS ULTRA55) after the samples were electro-polished with 10 % of perchloric acid (polishing voltage: 30 V, polishing time: 30 s, step size: 0.2 mm).

3 RESULTS AND DISCUSSION

3.1 Mechanical properties obtained with different aging processes

The engineering stress-strain curves of the studied steel obtained under different aging processes are given in **Figure 2a**. It can be easily observed that there is no apparent yield plateau on the tensile curves of all the samples processed with differnt aging processes, indicating that sufficient dislocations could be activated during the tensile deformation. Hence, the value of $\sigma_{p0.2}$ was determined to be the yield strength in this study, and the correlations between the tensile properties and aging temperature are depicted in **Figure 2b**. Following the variation trend of the tensile properties, there was a sharp decrease in the yield strength and tensile strength with the aging temperature increasing from 440 °C to 540 °C.

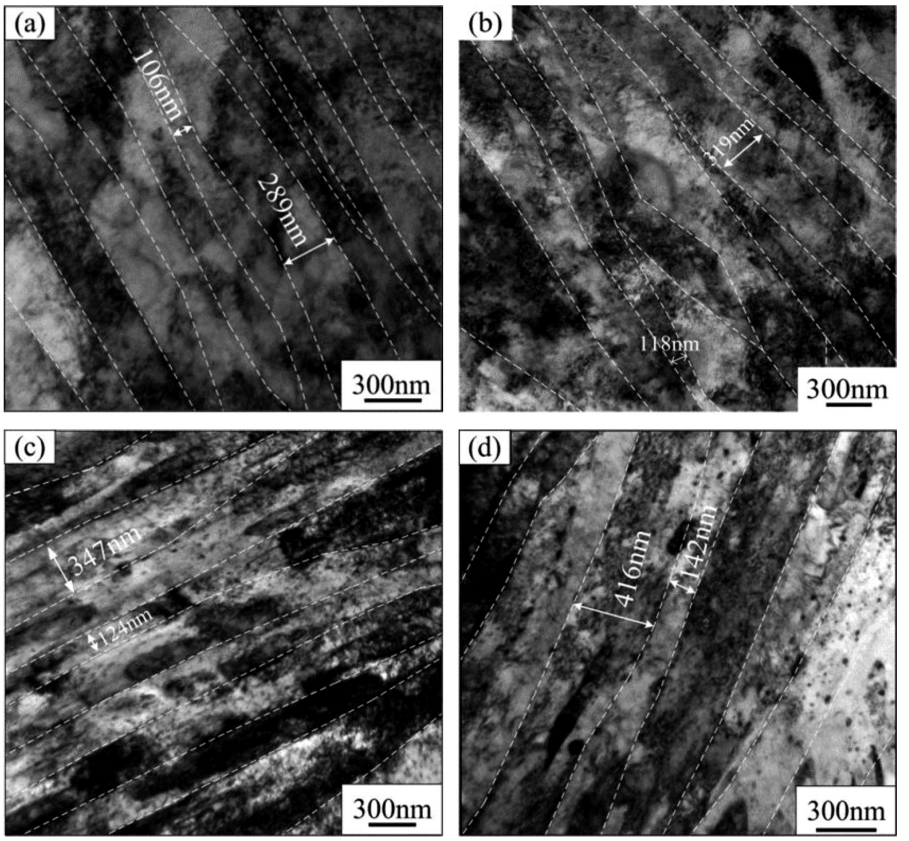

Figure 3: Substructure features obtained under aging temperatures of: a) 470 °C, b) 510 °C, c) 540 °C, d) 610 °C

Once the aging temperature was further increased to a range of 540–610 °C, the strength was first increased and then slightly decreased. The change in the fracture elongation maintained the opposite change relative to the strength, shown in **Figure 2b**. In summary, the lowest yield and tensile strengths obtained at 540 °C were determined to be ≈ 667 MPa and ≈ 979 MPa, respectively, compared to the other aging processes. In addition, more excellent comprehensive mechanical properties could be achieved with different aging processes such as the properties obtained at aging temperatures of (510, 570 and 610) °C, indicating a unique variation trend of the tensile properties of the studied steel, attributed to the specific microstructural feature and the difference between the strengthening mechanisms involved in different aging processes.

3.2 Microstructural features under different aging temperatures

Since the substructure of the martensite matrix could not be distinguished with optical microscopy due to a limited resolution, the micrographs obtained through TEM were therefore applied to characterize the microstructural features of the studied 15-5PH steel. **Figure 3** shows the substructure features of the studied steel obtained at an aging temperature range of 470–610 °C, including (470, 510, 540 and 610) °C, and it can be easily seen that the substructure of the studied steel is predominantly composed of lath martensite with different lath widths at all the processing conditions.

Generally, the precipitates formed on the ferrite matrix turned out to be predominantly Cu-enriched precipitates of the MSS,[8] and the second-phase strengthening mechanism induced by dispersed precipitates could play a significant role in contributing to the strength increment. The formation of the precipitates was also investigated in terms of the TEM characterization results, shown in **Figure 4**. In accordance with the analysis results, it can be understood that no precipitate was found on the ferrite matrix for the studied steel processed at the aging temperature of 470 °C, and a high density of dislocation cells could be observed on the ferrite matrix, as shown in **Figure 4a**. On the other hand, a large volume fraction of precipitates started to appear on the ferrite matrix once the aging temperature was increased to 510 °C, as shown in **Figure 4b**, and the dislocation cells could also be observed on the ferrite matrix. Once the aging temperature was increased to 540 °C and 610 °C, nano-sized precipitates with different shapes could also be found on the ferrite matrix, and an interaction trace between a precipitate and dislocation could also be observed, as shown in **Figures 4c** and **4d**. To further determine the composition of the nano-sized precipitates, a typical precipitate processed at 510 °C was selected for an energy spectrum analysis, which indicated that the

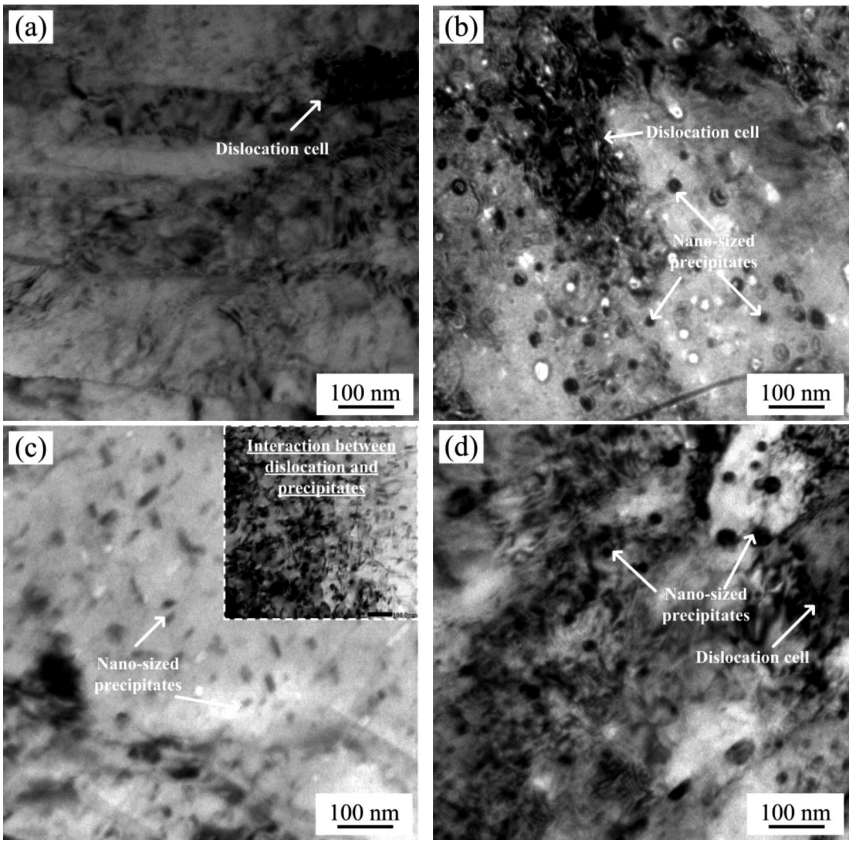

Figure 4: Precipitation morphology of the studied steel obtained at aging temperatures of: a) 470 °C, b) 510 °C, c) 540 °C, d) 610 °C

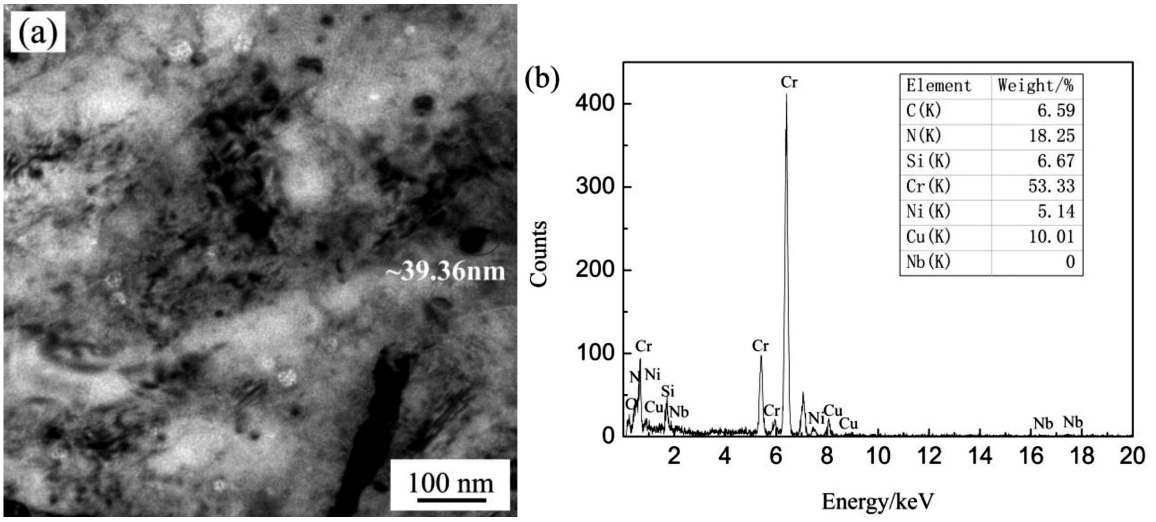

Figure 5: Energy spectrum analysis of typical precipitates distributed across the matrix of the studied steel processed at 510 °C

nano-sized particle was predominantly composed of C, N, Cu, Cr and Ni as shown in **Figure 5**.

In addition, the high density of dislocation cells could be locally observed on the ferrite matrix as shown in **Figures 3** and **4**. To explore the variation law of dislocation density under different aging temperatures, the kernal average misorientation (KAM) technique was applied to investigate the distribution feature of dislocations in a larger detection area. **Figure 6** shows the KAM analysis results for the studied steel processed at an aging temperature range of 470–610 °C, and it can be easily seen that the region with a high dislocation density or low dislocation density can be intuitively characterized, and the KAM distribution can be quantitatively described. The KAM analysis results indicate that the dislocation density at an aging temperature range of 410–540 °C varied slightly, and when the aging temperature was raised to 570 °C, there was an obvious increase associated with

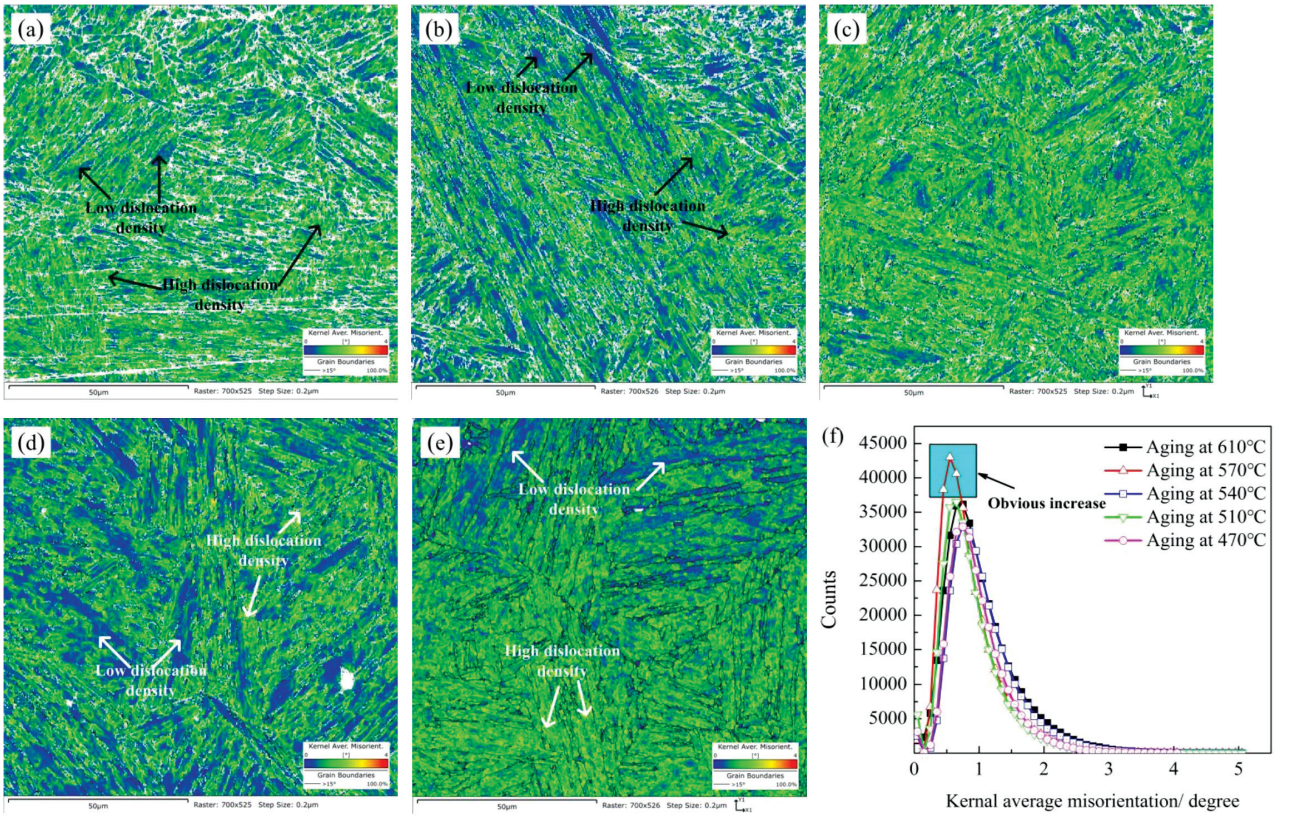

Figure 6: KAM analysis of the studied steel obtained at aging temperatures of: a) 470 °C, b) 510 °C, c) 540 °C, d) 570 °C, e) 610 °C, f) statistics data

Table 1: Expressions used for calculating the strength increments induced by different strengthening mechanisms

Expression	Equation No.	Reference
Relation between different strength increments: $\sigma_{P0.2} = \sigma_{SS} + \sigma_G + \sigma_D + \sigma_P$	1	10
Solid solution: $\sigma_{SS} = \sum_i [X_i]\sigma_{SSi} = 4570[C] + 37[Mn] + 83[Si] + 470[P] + 38[Cu] + 11[Mo] - 30[Cr]$	2	11
Grain refinement: $\sigma_G = \sigma_0 + K_{H-p} d^{-1/2}$	3	12
Precipitation: $\sigma_P = 0.3728 \frac{Gb}{1-v} \times \frac{\sqrt{f}}{d} \ln\left(\frac{1.2d}{2b}\right)$	4	13

the KAM distribution feature, indicating the dislocation density processed at the aging temperature of 570 °C was decreased significantly. On the other hand, the variation trend of dislocation density was unusual in terms of the traditional heat-treatment theory, and the dislocation density was increased when the aging temperature was further increased to 610 °C, as shown in **Figure 6f**.

Based on the experimental process and the equilibrium-phase transition diagram, it can be deduced that the inconsistent variation trend for the dislocation density and increasing aging temperatue was predominantly attributed to the reverse transformation of austenite. Once the aging temperature was raised to 570 °C, the large-area fraction of dislocation had to move, interact and disappear fastly, and the dislocation density began to decrease. In addition, the reverse transformation occurred and a certain volume fraction of fresh austenite could be achieved when the aging temperature was raised to 610 °C. Since the aging process allowed sufficient time for element partitioning from the ferrite matrix to fresh austenite, the achieved fresh austenite was stable. When the aging treatment continued, fresh austenite could be kept stable at a relatively low temperature region, and then again transformed into low-temperautre transformation products. Hence, the steel processed at the aging temperatue of 610 °C was characterized by high density of dislocations. In summary, it can be deduced that the density of dislocations was firstly decreased with the increasing aging temperature, and then it started to increase once the aging temperature was above the critical transformation temperature A_{C1}.

3.3 Variation in the strengthening mechanism at different aging temperatures

As stated in Section 3.2, the predominant microstructure feature was about the same for the studied 15-5PH steel under different aging processes. On the other hand, the precipitation behavior, distribution feature of dislocation density and lath width obtained at different aging processes were totally different considering the chemical composition and difference between the aging processes, indicating that the strengthening mechanisms involved in the studied steel were absolutely different. Hence, it was necessary to clarify the strengthening mechanism for the regulation of the microstructural features and mechanical properties of the studied 15-5PH steel. Generally, the strength contributions induced by different strengthening mechanisms including solid solution, grain size, dislocation and precipitation could be closely linked with each other and calculated through theoretical equations as shown in **Table 1**. When some typical interstitial or substitutional elements such as C, N, Mn were dissolved into the ferrite matrix, the solid-solution strengthening mechanism was generally active due to the differences in the atomic size and shear modulus between the dissolved atoms and matrix.[9] For the concrete chemical composition shown in Section 2, the strength contributions caused by solid-solution strengthening were calculated to be ≈ 32 MPa using Equation (2).

For grain refinement strengthening, the substructure of the studied steel obtained under different aging processes was characterized by lath martensite, and the martensite consisting of various kinds of packets, blocks and laths was transformed from the parent austenite. Since the block boundaries were generally classified as high-angle grain boundaries (HAGBs), they were expected to act as barriers for the moving dislocations during deformation.[14] The increase in the volume fraction of block boundaries caused by the grain refinement could lead to a strength increment for different ferrous steels.[15] The strength increments caused by grain refinement strengthening were achieved through the well-known Hall-Petch formula,[12] shown in Equation (3). In the present study, σ_0 was determined to be 50 MPa considering the similarity in the microstructure,[16] and the mean distance between any two adjacent block boundaries was regarded as the grain size d due to the hindering effect of the dislocation slip on the martensite microstructure. K_{H-P} was determined[13] to be 17.4 MPa·mm$^{1/2}$. The mean length between any two adjacent block boundaries of the studied steel aged at different temperatures were counted through EBSD images, and four random paths on the orientation map were selected to measure the boundary distance, as shown in **Figure 7**. The mean distances beween HAGBs corresponding to different aging processes were determined with the statistical analysis shown in **Figure 7**. The average distances between the HAGBs corre-

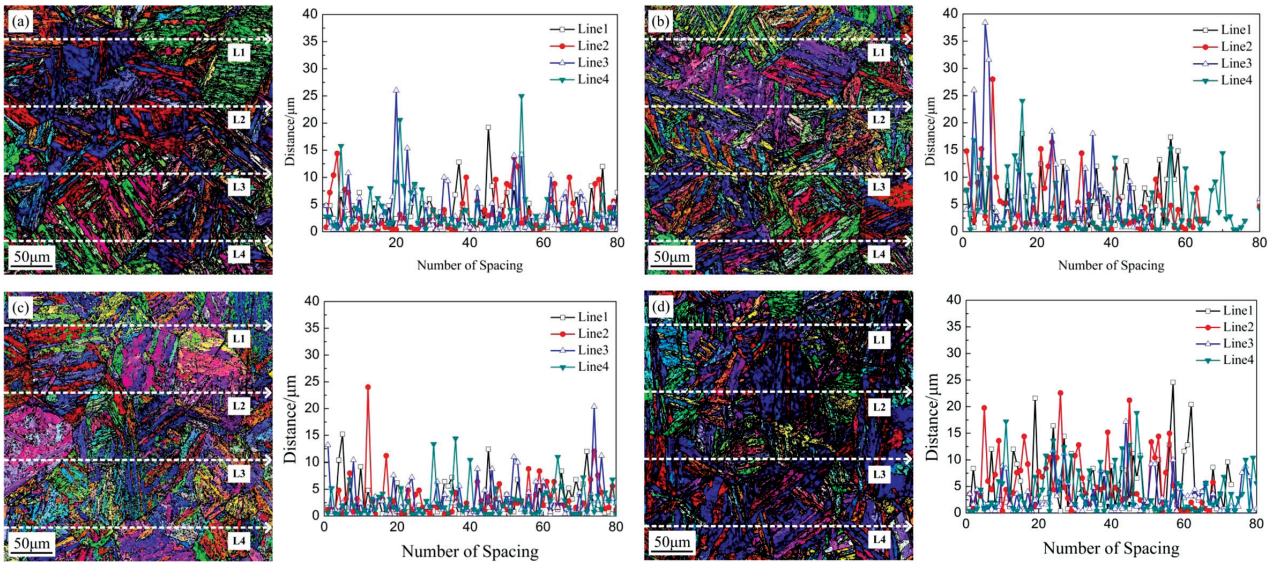

Figure 7: Orientation maps and the corresponding statistics for the distances between adjacent block boundaries processed at aging temperatures of: a) 470 °C, b) 510 °C, c) 540 °C, d) 610 °C

sponding to aging temperatures of (470, 510, 540 and 610) °C were determined to be (≈ 3.48, ≈ 5.02, ≈ 5.02 and ≈ 4.49) μm, respectively, and the strength contributions caused by the grain-refinement strengthening mechanism were estimated to be (≈ 345, ≈ 296, ≈ 296 and ≈ 310) MPa, respectively.

For 15-5PH stainless steel, it can be estimated that nanoscale precipitates should play a significant role in strengthening, considering a special alloying design feature, for example, the additions of Cu, Ni and Cr. As described in Section 3.2, some nanoscale Cu-enriched precipitates were found on the ferrite matrix processed at an

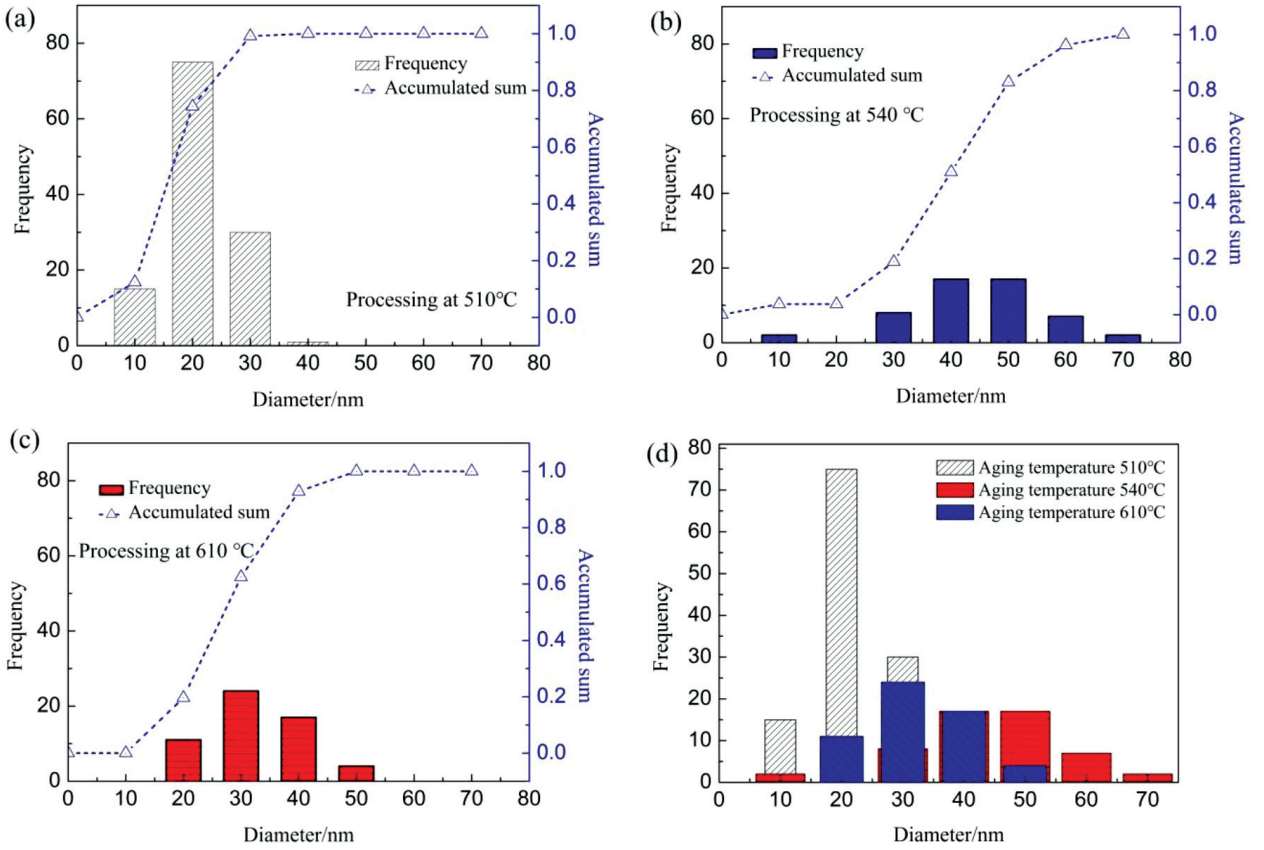

Figure 8: Distribution features of the precipitates obrtained through different aging processes: a) 510 °C, b) 540 °C, c) 610 °C, d) comparative analysis

aging temperature above 510 °C, and the precipitation strengthening could be predominant due to the apparent difference in crystal lattice between the Cu-enriched precipitation and the martensite matrix,[17] while the dislocation could be further obstructed and pinned effectively on the precipitated particles during the deformation, which further led to the strength increment.[18] The strengthening degree caused by the nanoscale precipitates depended on the particle size, volume fraction, lattice distortion of the matrix and particle, and the properties of precipitates.[19] Only a certain amount of nanoscale precipitates was achieved through a reasonable heat-treatment process, and the effective strengthening could be obtained. In this study, the strength contribution induced by precipitation strengthening was estimated with the Ashby-Orowan equation,[13] shown in Equation (4), while G, b and v were selected as 80 650 MPa, 0.248 nm and 0.291, respectively. Values of d and f were the average diameter and volume fraction of the precipitates, respectively, which were all measured through the TEM analysis.

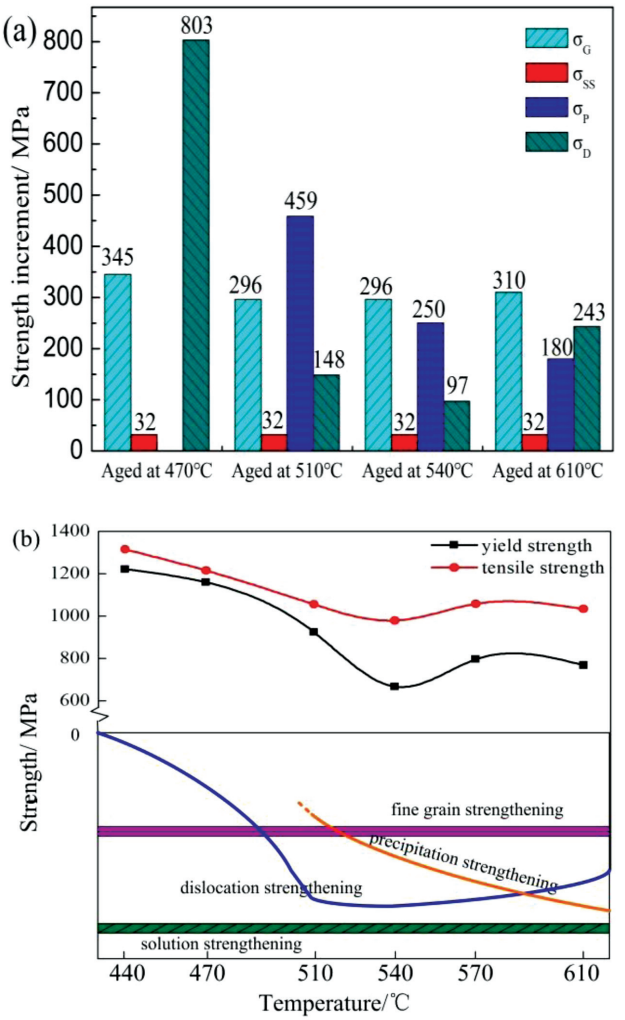

Figure 9: a) Comparison of the strength contributions caused by different strengthening mechanisms, and b) strengthening variation trend of the studied 15-5PH steel

Figure 8 shows the statistics of the precipitates obtained at aging temperatures above 510 °C, and six micrographs per processing condition were utilized for further analysis to make sure the statistics were representative. In accordance with the statistics, it could be concluded that the mean values of the precipitats corresponding to aging temperatures of (510, 540 and 610) °C were confirmed to be (≈ 14.08, ≈ 29.20 and ≈ 21.76) nm, respectively, and the area fractions were determiend to be ≈ 3.03 %, ≈ 2.66 % and ≈ 0.88 %, respectively. Considering the measurement operability, the area fraction was approximately applied to represent the volume fraction for further strength estimation, and the strength increments induced by the precipitation strengthening mechanism at (510, 540 and 610) °C were calculated to be (≈ 458.51, ≈ 250.06 and ≈ 179.7) MPa, respectively.

The dislocation strengthening mechanism also played a significant role in the strength increment of the studied steel due to the substructure feature of lath martensite, indicating that dislocation strengthening was dominant at a certain temperature. The entanglement of dislocations increased the resistance of dislocation movement, which inevitably contributed to the strength increment.[20] In this study, the strength increment induced by dislocation strengthening was further calculated by excluding the strength contributions induced by the other strengthening mechanisms from the yield strength, and the strength contributions corresponding to aging temperatures of (470, 510, 540 and 610) °C were determined to be (803, 148, 97 and 243) MPa, respectively.

Table 2: Strength increments induced by different strengthening mechanisms

Aging process (°C)	$\sigma_{p0.2}$ (MPa)	Solid-solution strengthening (MPa)	Grain-refinement strengthening (MPa)	Dislocation strengthening (MPa)	Precipitation strengthening (MPa)
470	1180	32	345	803.00	0.00
510	935	32	296	148.49	458.51
540	675	32	296	96.94	250.06
610	765	32	310	243.30	179.70

In summary, the strength contributions induced by different strengthening mechanisms for the studied 15-5PH steel are comparatively shown in **Table 2** and **Figure 9a**. It can be concluded that the strength contributions induced by grain-refinement strengthening and solid-solution strengthening remained nearly stable with the varied aging temperature, and the strength contribution induced by the grain-refinement strengthening mechanism was distributed in a strength range of 296–345 MPa, corresponding to an aging temperature range of 470–610 °C. On the other hand, the role of the dislocation strengthening mechanism varied significantly under different aging temperatures in strengthening the

steel, and the strength increments caused by the dislocation strengthening mechanism were distributed across a wide strength range of 97–803 MPa. Similarly, the strength increments induced by the precipitation strengthening mechanism were distributed across a wide strength range of 0–469 MPa, indicating that the precipitation-strengthening effect was sensitive to the change in the aging temperature. The variation trend of the strengthening mechanism can be further understood through **Figure 9b**. Although similar mechanical properties obtained with different aging processes can be achieved, the strengthening mechanisms of the steel were absolutely different, and the strength increments caused by different combinations of precipitation strengthening and dislocation strengthening were crucial for determining the final mechanical properties of the studied 15-5PH stainless steel.

4 CONCLUSIONS

For the studied 15-5PH steel, the tensile strength was decreased with an aging temperature increase from 440 °C to 540 °C; the strength was first increased followed by a slight decrease once the aging temperature was further increased to an aging temperature range of 540–610 °C. The variation in the fracture elongation kept an opposite variation trend relative to the variation in the tensile strength over the whole aging temperature range of 440–610 °C.

The strength increments induced by grain-refinement strengthening and solid-solution strengthening remained nearly stable with the varied aging temperature. The strength increment caused by the grain-refinement strengthening mechanism was distributed in a strength range of 296–345 MPa, corresponding to the aging temperature range of 470–610 °C, and the strength increments caused by dislocation strengthening and precipitation strengthening were determined to be distributed in strength ranges of 97–803 MPa and 0–469 MPa, respectively.

The strength increments induced by different combinations of precipitation strengthening and dislocation strengthening were crucial for determining the final mechanical properties of the studied 15-5PH stainless steel.

Acknowledgement

The authors acknowledge the financial support from the Outstanding Doctoral Award for Work in Shanxi, China (No. 20192041) and Applied Basic Research Program in Shanxi, China (No. 201901D211309). J. S. Chen appreciates the support from the National Natural Science Foundation of China (No. 51904156).

5 REFERENCES

[1] S. Ifergane, M. Pinkas, Z. Barkay, E. Brosh, V. Ezersky, O. Beeri, N. Eliaz, The relation between aging temperature, microstructure evolution and hardening of Custom 465 stainless steel, Mater. Charact., 127 (**2017**), 129–136, doi:10.1016/j.matchar.2017.02.023

[2] W. Xu, P. E. J. Rivera-Díaz-del-Castillo, W. Yan, K. Yang, D. San Martin, L. A. I. Kestens, S. van der Zwaag, A new ultrahigh-strength stainless steel strengthened by various coexisting nanoprecipitates, Acta Mater., 58 (**2010**) 11, 4067–4075, doi:10.1016/j.actamat.2010.03.005

[3] Z. Wang, L. Hui, S. Qin, W. Liu, Z. Wang, Nano-precipitates evolution and their effects on mechanical properties of 17-4 precipitation-hardening stainless steel, Acta Mater., 156 (**2018**), 158–171, doi:10.1016/j.actamat.2018.06.031

[4] D. Palanisamy, P. Senthil, V. Senthilkumar, The effect of aging on machinability of 15Cr–5Ni precipitation hardened stainless steel, Arch. Civ. Mech. Eng., 16 (**2016**) 1, 53–63, doi:10.1016/j.acme.2015.09.004

[5] K. S. Chenna, N. K. Gangwar, A. K. Jha, B. Pant, K. M. George, Microstructure and properties of 15Cr-5Ni-1Mo-1W martensitic stainless steel, Steel Res. Int., 86 (**2015**) 1, 51–57, doi:10.1002/srin.201400035

[6] C. H. Jin, H. L. Zhou, Y. Lai, B. Li, K. W. Zhang, H. Q. Chen, J. H. Zhao, Microstructure and mechanical properties of 15-5 PH stainless steel under different aging temperature, Metall. Res. Technol., 118 (**2021**) 6, doi:10.1051/metal/2021078

[7] S. H. Zhang, L. Deng, L. Z. Che, An integrated model of rolling force for extra-thick plate by combining theoretical model and neural network model, J. Manuf. Process, 75 (**2022**), 100–109, doi:10.1016/j.jmapro.2021.12.063

[8] X. Y. Peng, X. L. Zhou, X. Z. Hua, Z. W. Wei, H. Y. Liu, Effect of aging on hardening behavior of 15-5 PH stainless steel, J. Iron Steel Res., 22 (**2015**) 7, 607–614, doi:10.1016/S1006-706X(15)30047-9

[9] C. R. Hutchinson, J. F. Nie, S. Gorsse, Modeling the precipitation processes and strengthening mechanisms in a Mg-Al-(Zn) AZ91 alloy, Metall. Mater. Trans. A, 36 (**2005**) 8, 2093–2105, doi:10.1007/s11661-005-0330-x

[10] H. K. D. H. Bhadeshia, Models for the elementary mechanical properties of steel welds, Mathematical modelling of weld phenomena III, Institute of Materials, London, 1997, 229

[11] Q. L. Yong, Secondary phases in steels, Metallurgical Industry Press, Beijing, 2006, 7

[12] E. O. Hall, The deformation and ageing of mild steel: III Discussion of results, Proceedings of the Physical Society, 643 (**1951**) 9, 747–752, doi:10.1088/0370-1301/64/9/303

[13] M. X. Sun, Y. Xu, W. B. Du, Influence of coiling temperature on microstructure, precipitation behaviors and mechanical properties of a low carbon Ti micro-alloyed steel, Metals (Basel), 10 (**2020**) 9, 1173, doi:10.3390/met10091173

[14] S. Morito, H. Yoshida, T. Maki, X. Huang, Effect of block size on the strength of lath martensite in low carbon steels, Mater. Sci. Eng. A, 438 (**2006**) 1, 237–240, doi:10.1016/j.msea.2005.12.048

[15] T. Huang, C. Li, G. Wu, T. Yu, Q. Liu, N. Hansen, X. Huang, Particle stabilization of plastic flow in nanostructured Al-1 %Si Alloy, J. Mater. Sci., 49 (**2014**) 19, 6667–6673, doi:10.1007/s10853-014-8338-5

[16] L. Yue, L. Zhou, Y. Jiang, Y. Zhang, Z. Zhou, L. Qian, The microstructure evolution and properties of a Cu–Cr–Ag alloy during thermal-mechanical treatment, J. Mater. Res., 32 (**2017**) 7, 1324–1332, doi:10.1557/jmr.2017.17

[17] R. Monzen, M. L. Jenkins, A. P. Sutton, The bcc-to-9R martensitic transformation of Cu precipitates and the relaxation process of elastic strains in an Fe-Cu alloy, Philos. Mag., 80 (**2000**) 3, 711–723, doi:10.1080/01418610008212077

[18] M. P. Baranivsky, A. I. Katsman, N. Devčić, Precipitation hardening in metals, 10th International Symposium of Croatian Metallurgical Society, SHMD, Šibenik, 2012

[19] L. Peng, H. Xie, G. Huang, G. Xu, X. Yin, X. Feng, X. Mi, Z. Yang, The phase transformation and strengthening of a Cu-0.71wt% Cr alloy, J. Alloys Compd., 708 (**2017**) 1096–1102, doi:10.1016/j.jallcom.2017.03.069

[20] L. M. Cheng, W. J. Poole, J. D. Embury, D. J. Lloyd, The influence of precipitation on the work-hardening behavior of the aluminum alloys AA6111 and AA7030, Metall. Mater. Trans. A, 34 (**2003**) 11, 2473–2481, doi:10.1007/s11661-003-0007-2